

Supplementary Figure 1

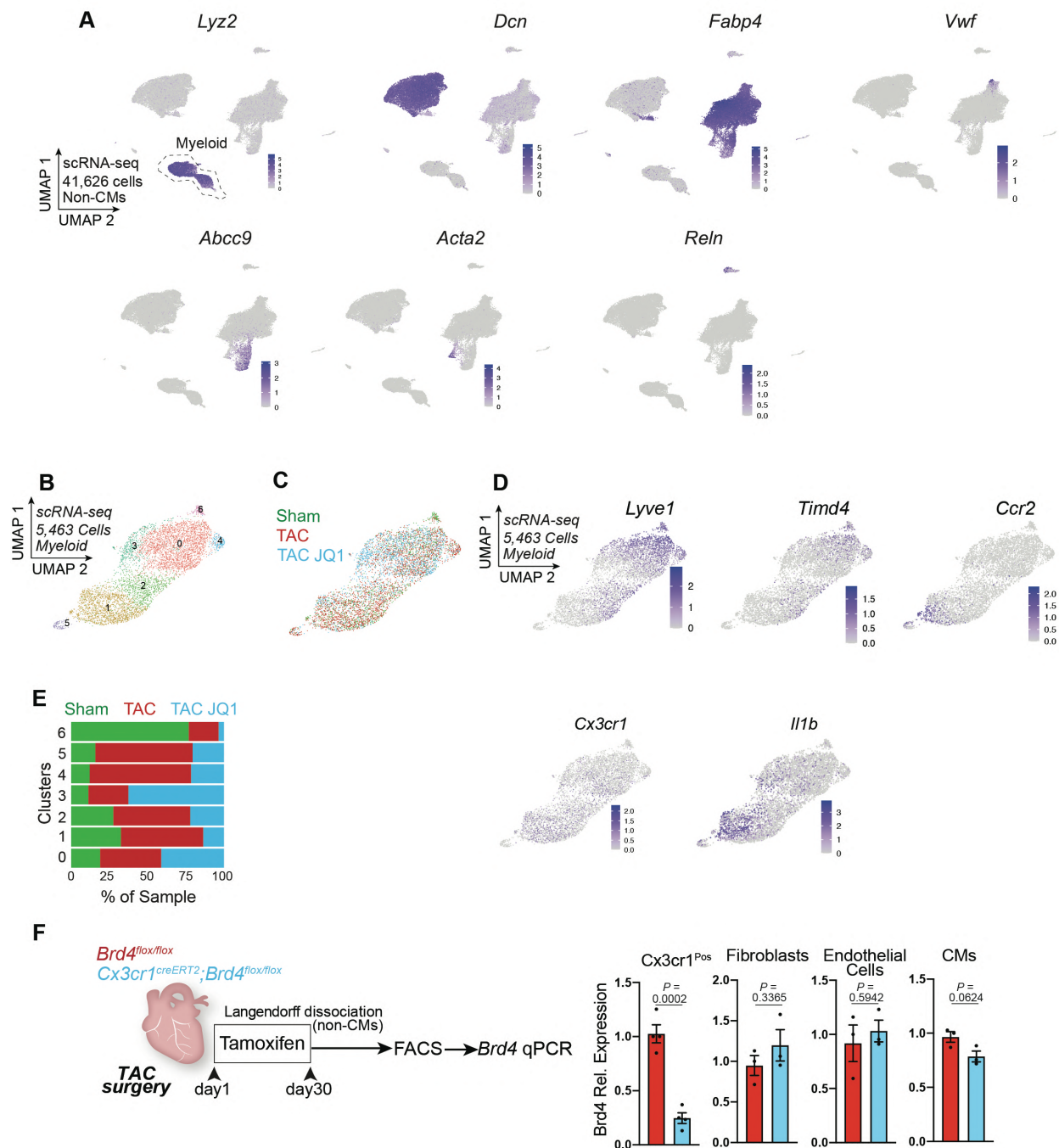


Figure S1: Single-cell RNA-seq in heart failure with BET inhibition identifies a highly dynamic *Cx3cr1*-expressing monocyte/macrophage subpopulation

A. Expression Feature Plots (scRNA-seq) of cell population markers in non-CM cells. **B,C.** UMAP plot (scRNA-seq) of myeloid cells colored by cluster (B) and sample identity (C). **D.** Expression Feature Plots (scRNA-seq) of *Lyve1*, *Timd4*, *Ccr2*, *Cx3cr1* and *Il-1b* in myeloid cells. **E.** Sample distribution within clusters in myeloid cells. **F.** Schematic of experimental settings for conditional *Brd4* deletion in *Cx3cr1*^{Pos} cells. *Brd4* expression was measured by qPCR in sorted *CX3CR1*^{Pos}, fibroblasts (*mEF-SK4*^{Pos}, *CD45*^{Neg}, *CD31*^{Neg}), endothelial cells (*mEF-SK4*^{Neg}, *CD45*^{Neg}, *CD31*^{Pos}) and in unsorted CMs. **F.** Data are mean ± s.e.m. Unpaired, two-tailed Student's *t*-test.

Supplementary Figure 2

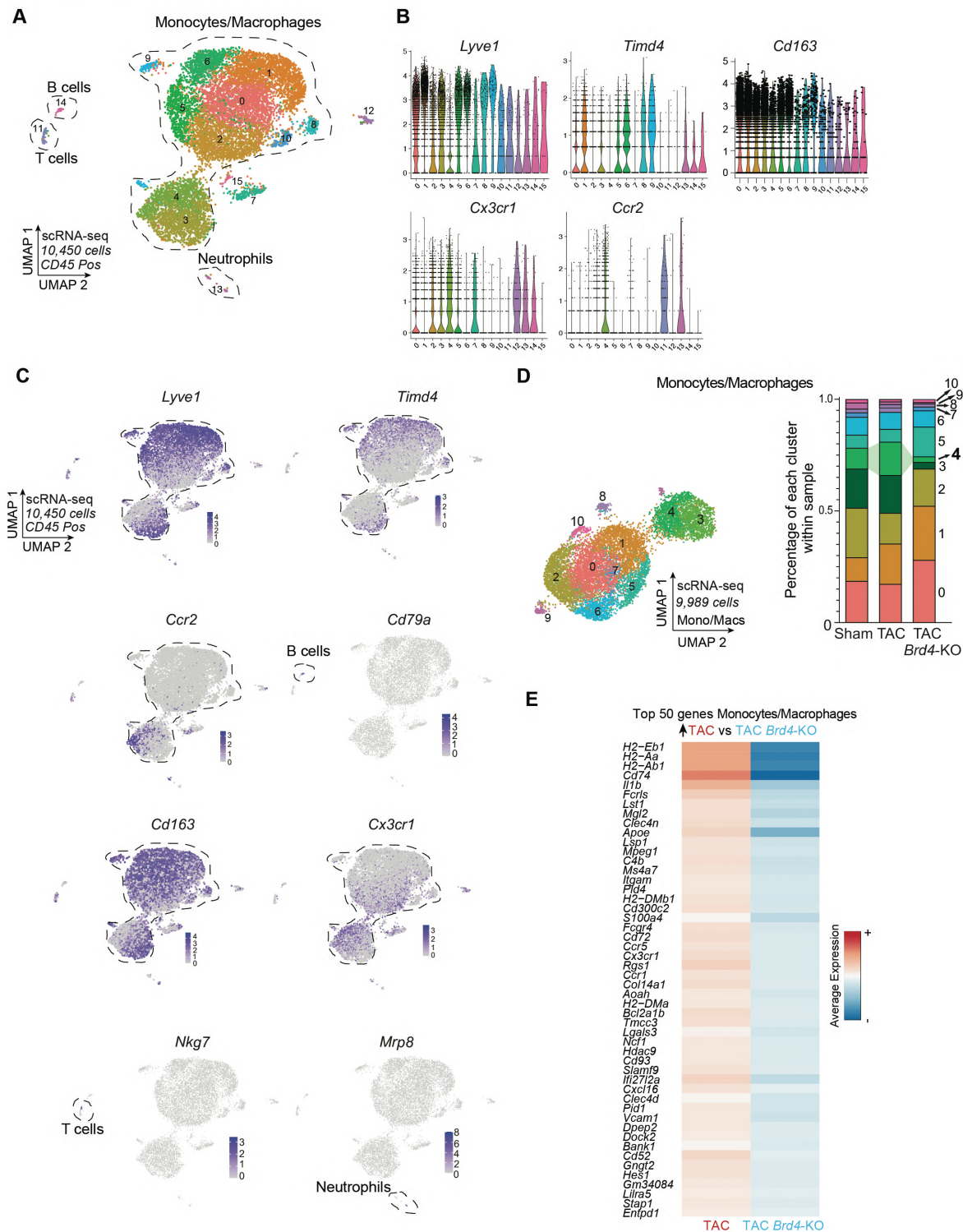


Figure S2: Identification of monocyte/macrophage population with single-cell RNA-seq

A. UMAP plot (scRNA-seq) of CD45^{Pos} cells colored by cluster identity. **B.** Expression Violin Plots of *Lyve1*, *Timd4*, *Cd163*, *Cx3cr1* and *Ccr2* in CD45^{Pos} cells. **C.** Expression Feature Plots (scRNA-seq) of *Lyve1*, *Timd4*, *Ccr2*, *Cd79a*, *Cd163*, *Cx3cr1*, *Nkg7* and *Mrp8* in CD45^{Pos} cells. **D.** UMAP plot (scRNA-seq) of monocytes/macrophages colored by cluster (left) and cluster composition within samples (right). Changes in cluster 4 are highlighted. **E.** Heatmap of expression (scRNA-seq) depicting the top 50 genes upregulated in TAC versus TAC Brd4-KO in the monocyte/macrophage population.

Supplementary Figure 3

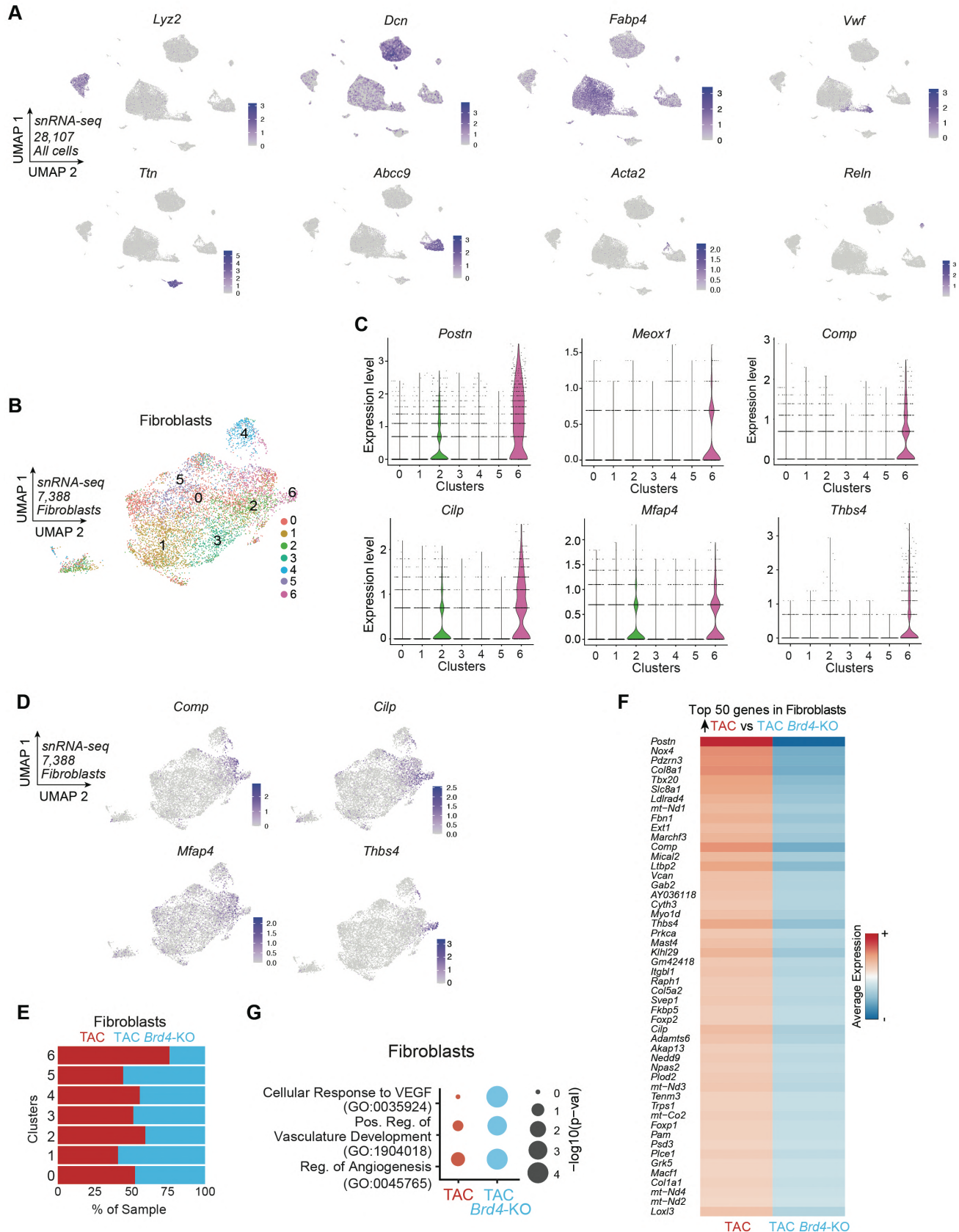


Figure S3: Decreased profibrotic signature in fibroblasts with Brd4 deletion in Cx3cr1-expressing monocytes/macrophages.

A. Expression Feature Plots (snRNA-seq) of cell population markers in nuclei from cardiac tissue. **B.** UMAP plot (snRNA-seq) of fibroblasts colored by cluster identity. **C.** Expression Violin Plots (snRNA-seq) of *Postn*, *Meox1*, *Comp*, *Cilp*, *Mfap4* and *Thbs4* across clusters in fibroblasts. **D.** Expression Feature Plots (snRNA-seq) of *Comp*, *Cilp*, *Mfap4* and *Thbs4* in fibroblasts. **E.** snRNA-seq sample distribution within fibroblast clusters. **F.** Heatmap of expression (snRNA-seq) depicting the top 50 genes upregulated in TAC versus TAC Brd4-KO in fibroblasts. **G.** Dot Plot indicating significance ($-\log_{10}(p\text{-val})$) for indicated GO terms in genes upregulated in TAC vs TAC Brd4-KO (red) or upregulated in TAC Brd4-KO vs TAC (blue) in fibroblasts.

Supplementary Figure 4

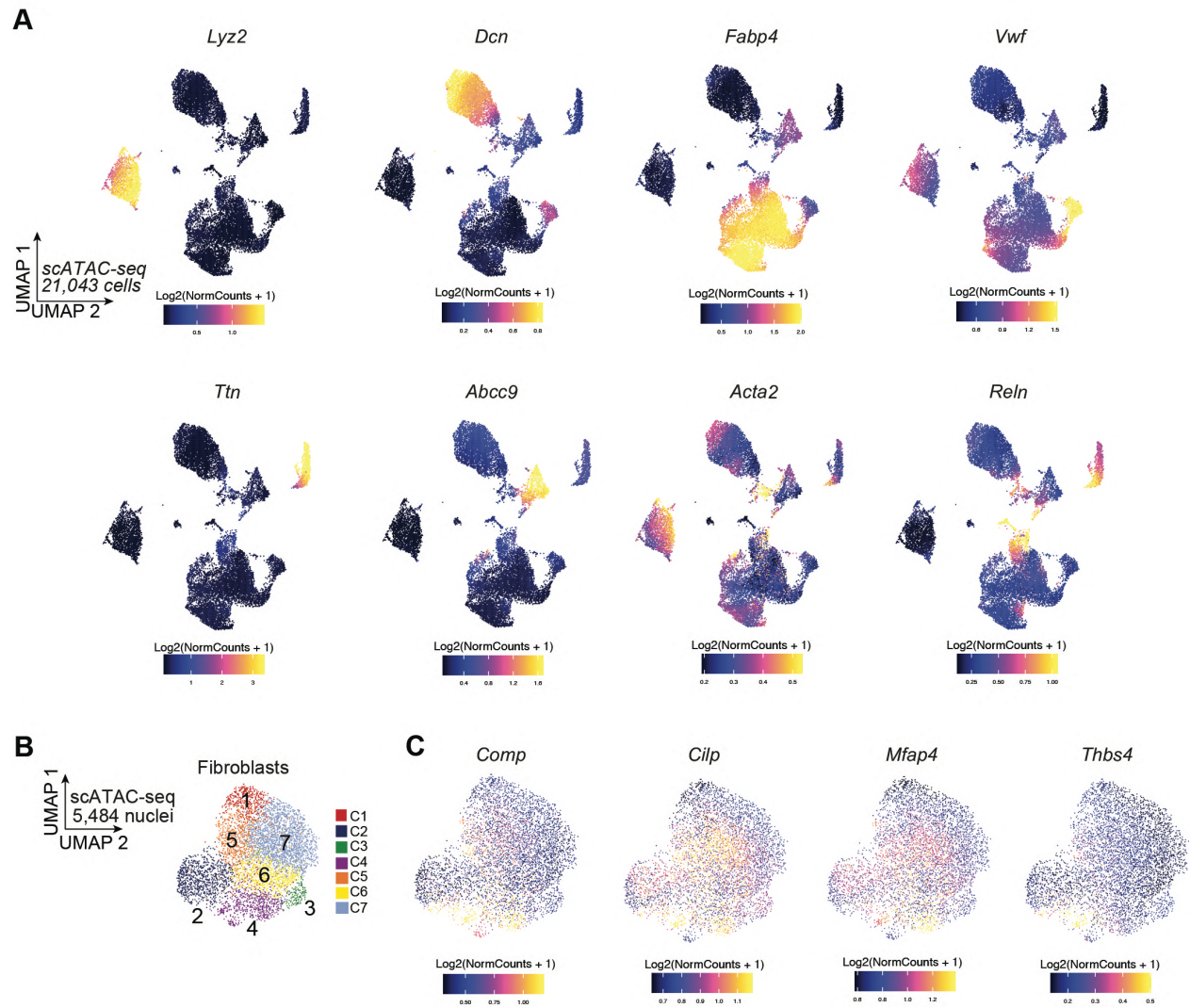


Figure S4: Changes in fibroblast chromatin accessibility with *Brd4* deletion in *Cx3cr1*-expressing monocytes/macrophages

A. Chromatin accessibility gene score of cell population markers across nuclei from cardiac tissue. **B.** UMAP plot (scATAC-seq) of fibroblasts colored by cluster identity. **C.** Chromatin accessibility gene score of *Comp*, *Cilp*, *Mfap4* and *Thbs4* in fibroblasts.

Supplementary Figure 5

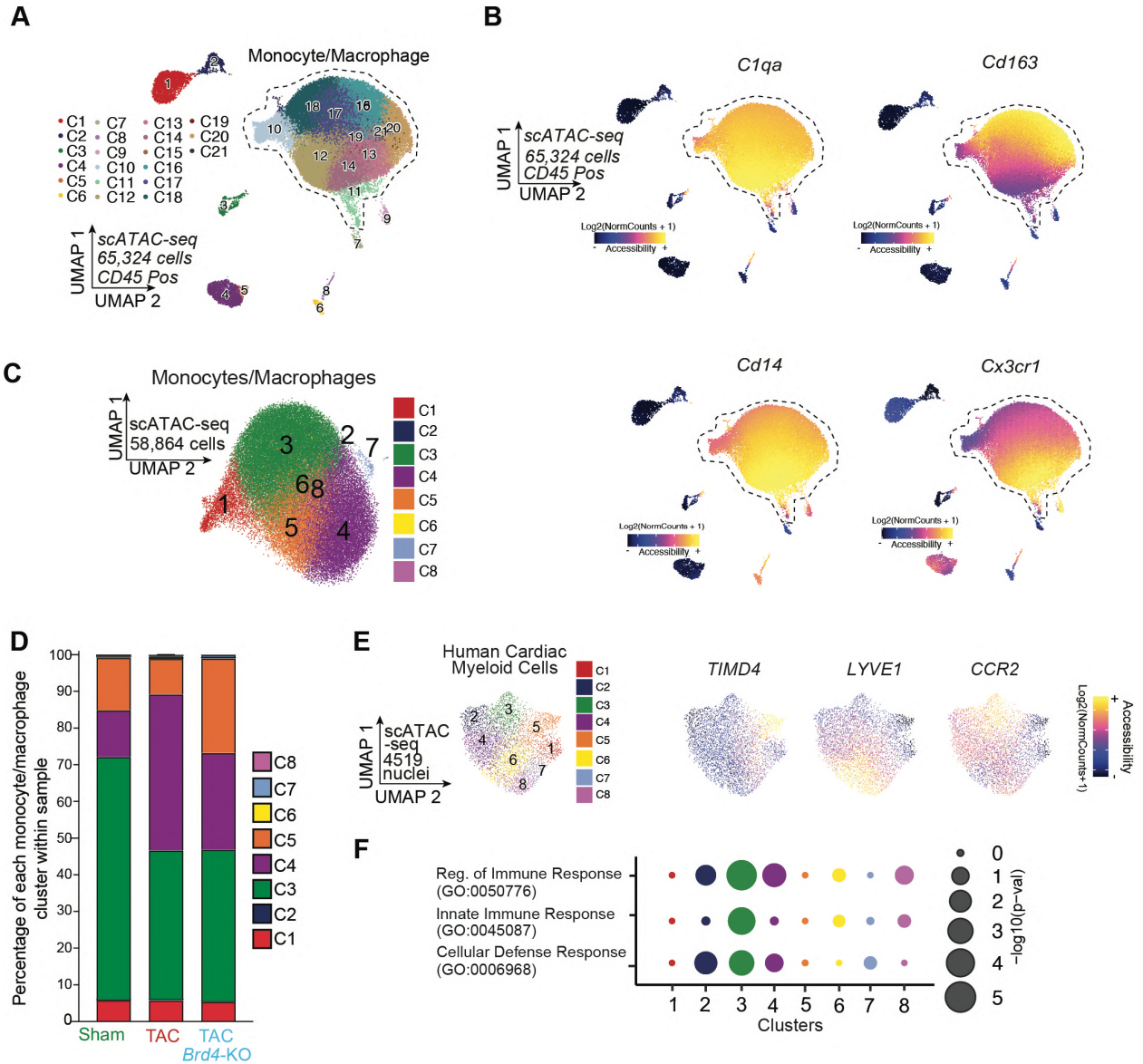


Figure S5: Identification of monocyte/macrophage population with single-cell ATAC-seq

A. UMAP plot (scATAC-seq) of CD45^{Pos} cells colored by cluster, the clusters encompassing the monocyte/macrophage populations are highlighted. **B.** Chromatin accessibility gene score of *C1qa*, *Cd163*, *Cd14* and *Cx3cr1* in CD45^{Pos} cells. **C.** UMAP plot (scATAC-seq) of monocytes/macrophages colored by cluster identity. **D.** Monocyte/macrophage cluster distribution within samples. **E.** Chromatin accessibility gene score of *TIMD4*, *LYVE1* and *CCR2* in human cardiac myeloid cells. **F.** Dot Plot indicating significance ($-\log_{10}(p\text{-val})$) for indicated GO terms across human myeloid cell clusters.

Supplementary Figure 6

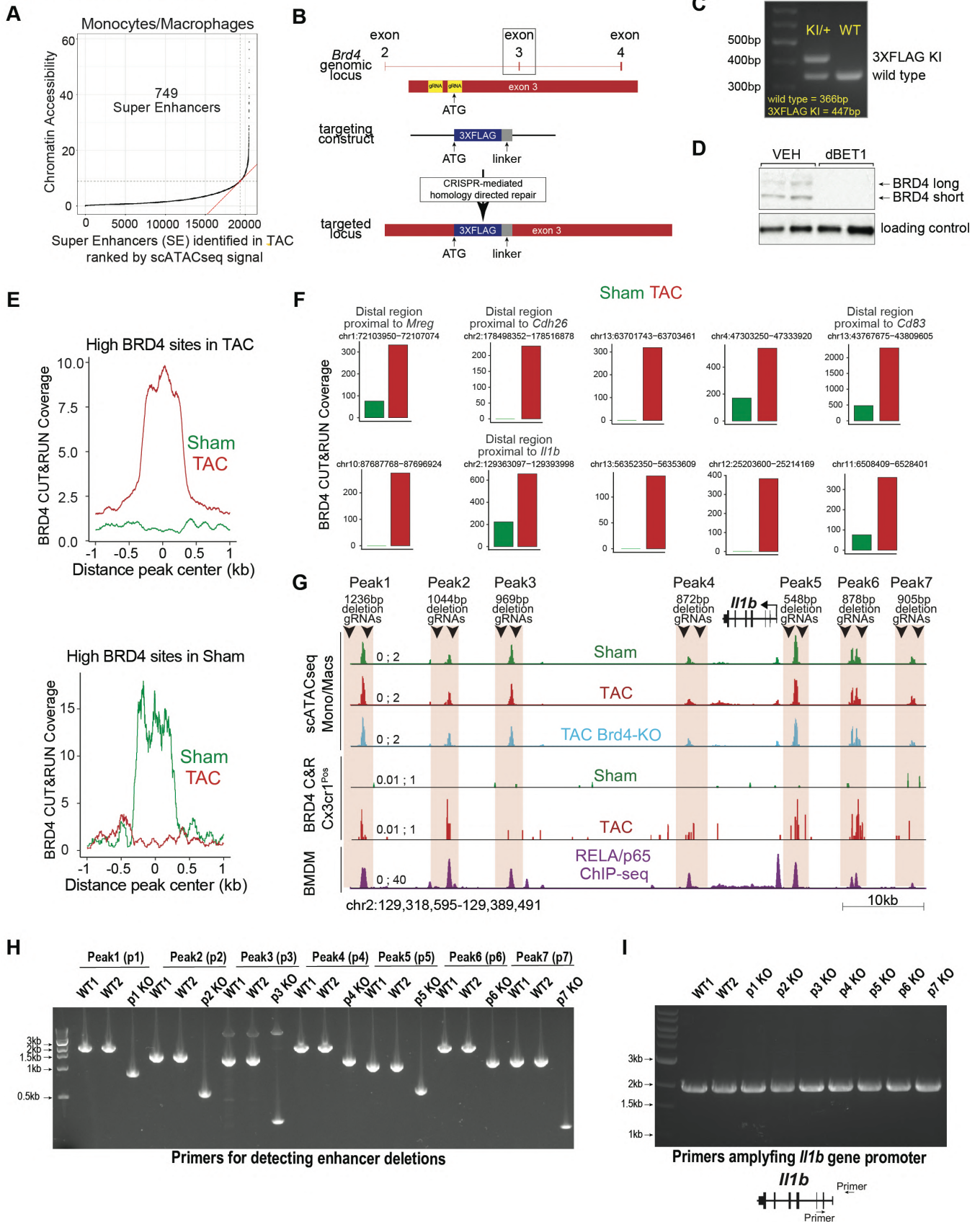


Figure S6: Chromatin accessibility and BRD4 occupancy in Cx3cr1-expressing cells identifies set of highly dynamic monocytes/macrophages distal elements in heart failure

A. Distribution of accessibility in monocytes/macrophages in the TAC state identifies a class of distal regions (super-enhancers (SE)) for which the accessibility falls over the inflection point of the curve. **B.** Schematic of the targeting strategy to generate the *Brd4* 3xFlag mouse. **C.** Western blot showing WT and 3xFLAG knock-in bands in WT and *Brd4*^{flag/+} animals. **D.** Liver tissue western blot showing expression of endogenous long and short BRD4 isoforms treated with vehicle or with the small-molecule BET protein degrader dBET1⁴⁰. **E.** Coverage from anti-FLAG Cut&Run in Sham and TAC identifies regions enriched with BRD4 in stress (left) or at baseline (right). **F.** Coverage from anti-FLAG CUT&RUN in Sham and TAC in selected ten super enhancer regions. **G.** Schematic of the *Il1b* locus displaying the location of the gRNAs used to delete the 7 distal regions (Peak1 to Peak7). **H,I.** Agarose gel electrophoresis to assess distal peak deletions in *Il1b* locus (H) and unaffected region around *Il1b* promoter (I) (1813bp) in WT and KO clones.

Suppl Figure 7

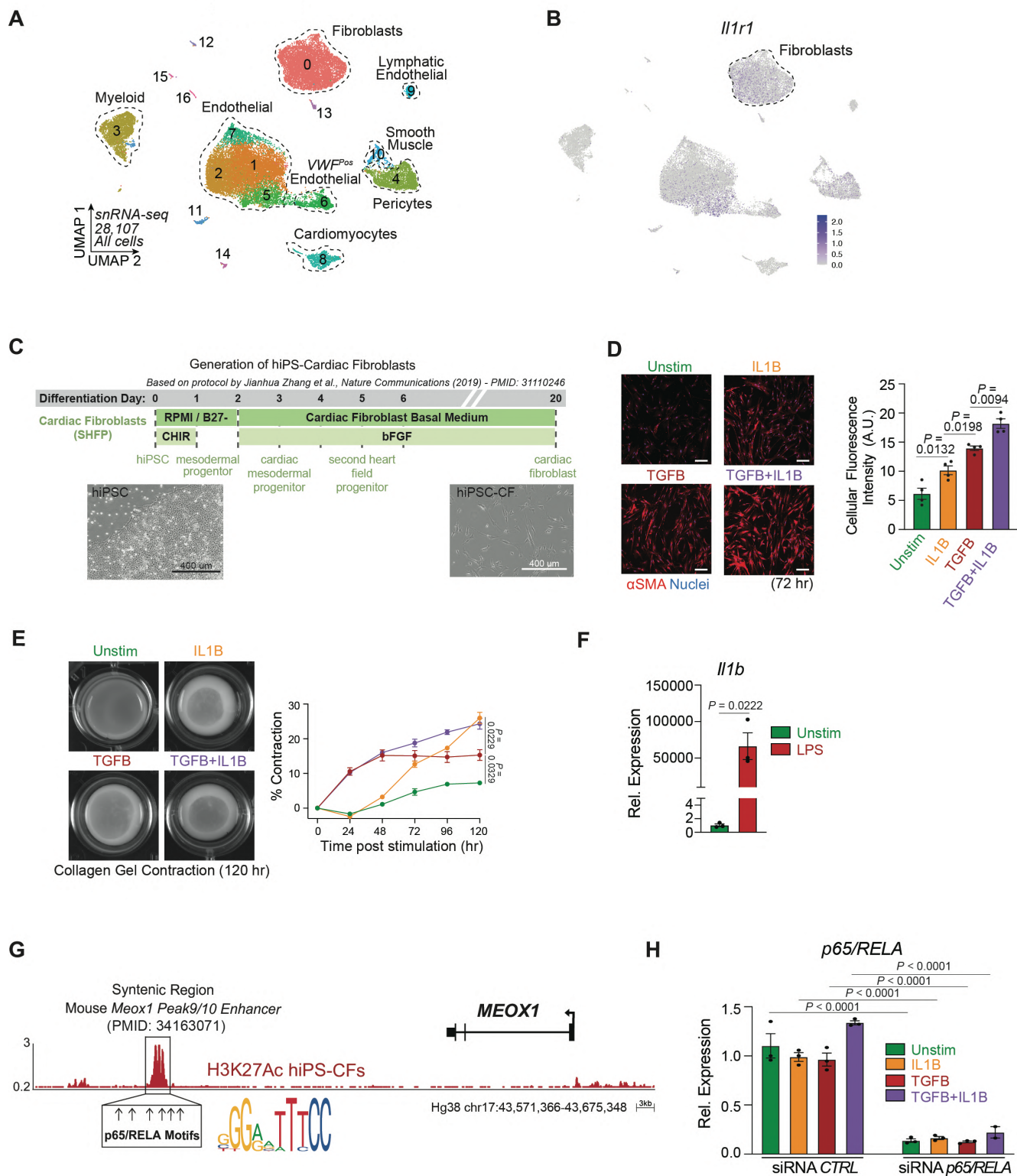


Figure S7: IL1B increases profibrotic response in human induced pluripotent cardiac fibroblasts

A. UMAP plot (snRNA-seq) of nuclei from cardiac tissue colored by cluster identity. **B.** Expression Feature Plot of *Il1r1* in nuclei from cardiac tissue. Fibroblasts are highlighted. **C.** Protocol to generate human induced pluripotent cardiac fibroblasts (iPS-CFs). **D.** Immunofluorescence staining of α SMA (left) in Unstimulated iPS-CFs or treated with IL1B, TG-B or TGFB+IL1B. Nuclei are marked by Hoechst. Scale bars, 200 μ m. Right, quantification of α SMA staining. **E.** Images (left) and quantification (right) of iPS-CFs seeded on compressible collagen gel matrices in unstimulated or with IL1B, TGFB or TGFB+IL1B treatments. **F.** *Il1b* expression by qPCR in Unstimulated and LPS treated Raw264-7 macrophages. **G.** Human *MEOX1* locus showing H3K27Ac in unstimulated iPS-CFs. The syntenic region of the mouse *Meox1* Peak9/10 regulatory element³ is highlighted and the six p65/RELA motifs within the region indicated. **H.** p65/RELA expression by qPCR in Unstimulated iPS-CFs or treated with IL1B, TGFB or TGFB+IL1B with control or p65/RELA-targeting siRNAs. **D-F,H** Data are mean \pm s.e.m. One-way (D,H) and Two-way (E) ANOVA followed by Tukey post hoc test. Unpaired, two-tailed Student's *t*-test (F).

Supplementary Figure 8

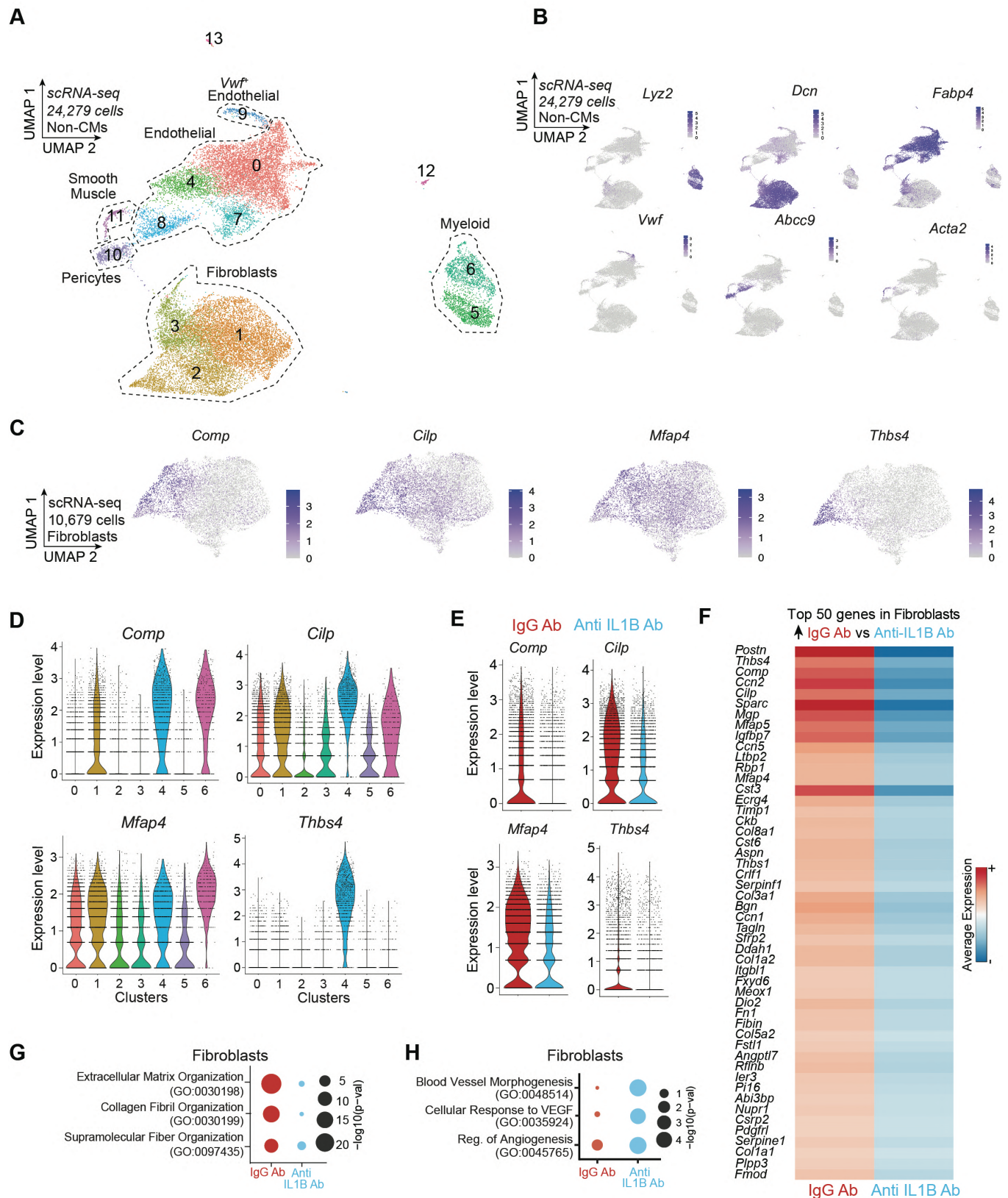


Figure S8: In vivo antibody-mediated IL1B neutralization decreases profibrotic transcriptional signature in fibroblasts

A. UMAP plot (scRNA-seq) of non-cardiomyocyte cells colored by cluster. **B** Expression Feature Plots (scRNA-seq) of cell population markers in non-cardiomyocyte cell population. **C.** Expression Feature Plots (scRNA-seq) of *Comp*, *Cilp*, *Mfap4* and *Thbs4* in fibroblasts. **D.** Expression Violin Plots (scRNA-seq) of *Comp*, *Cilp*, *Mfap4* and *Thbs4* across clusters in fibroblasts. **E.** Expression Violin Plots (scRNA-seq) of *Comp*, *Cilp*, *Mfap4* and *Thbs4* across samples in fibroblasts. **F.** Heatmap of expression (scRNA-seq) depicting the top 50 genes upregulated in TAC IgG Ab versus TAC Anti-IL1B Ab in fibroblasts. **G,H.** Dot Plot indicating significance ($-\log_{10}(p\text{-val})$) for indicated GO terms in genes upregulated in IgG vs Anti-IL1B (red) or upregulated in Anti-IL1B vs IgG (blue) in fibroblasts.